Numerical Simulation on Influencing Factors of Co-firing of Municipal Solid Waste and Leather

Huang Guo,[a] Baojun Yi,[a,b,*] Hongpeng Xu,[c] Lu Dong,[d] Guangzhao Guo,[e] and Lifang Gong [e]

Incineration is an important method of recycling municipal solid waste (MSW). As an industrial waste, leather has a higher calorific value and more combustible components than MSW. The blending of leather can make up for the high moisture content and insufficient calorific value of MSW, providing a good solution to reduce the capacity of MSW and industrial waste. This study predicts the effect of blending combustion by means of numerical simulation; the effects of leather blending ratio, the ratio of primary air and secondary air, total air volume, and fuel feed rate were analyzed. The results showed that the appropriate increase of blending ratio improves the furnace chamber temperature, and the best blending amount of leather is approximately 10%. The best primary and second air ratio is 0.72:0.28. Insufficient airflow caused inadequate combustion, and excessive airflow reduced the furnace temperature. The feed volume in the range of 500 to 550 t/d had a good burning effect.

DOI: 10.15376/biores.18.2.3666-3680

Keywords: Incineration; Municipal solid waste; Leather; Co-firing; Simulation

*Contact information: a: College of Engineering, Huazhong Agricultural University, Wuhan, 430070, China, No. 1, Shizishan Street, Hongshan District, Wuhan, 430070, Hubei Province, P. R. China; b: Key Laboratory of Smart Farming for Agricultural Animals, Ministry of Agriculture and Rural Affairs, Huazhong Agricultural University, Wuhan, 430070, Hubei Province, P. R. China; c: College of Vehicle and Energy, Yanshan University, Qinhuangdao, 066004, China; d: State Key Laboratory of Coal Combustion, Huazhong University of Science and Technology, Wuhan, 430074, China; e: Grandblue Environment Corporation, Foshan, 528299, China; *Corresponding authors: bjyi@mail.hzau.edu.cn*

INTRODUCTION

Rapid economic development and urbanization has increased the production of municipal solid waste (MSW). Incineration reduces the volume of MSW by 85% and provides a solution to problems such as waste odor and leachate (Martin *et al.* 2015; Lopes *et al.* 2018; Duan *et al.* 2020). Yan *et al.* (2021) simulated the influence of multi-temperature primary air on the characteristics of MSW; compared with preheated primary air, the multi-temperature effectively controls the temperature of the generated gas and peak furnace temperature. Gu *et al.* (2022b) adjusted the primary air distribution, enhancing the reaction with NH_3 and coke results in lower NO_x emission.

As an industrial waste, leather has a high organic matter content, and its direct combustion will cause serious pollution to the environment; therefore, the sustainable treatment of industrial waste is particularly important (Muralidharan *et al.* 2022). Zhang *et al.* (2022) studied the co-combustion process of tannery waste and found that parameters such as integrated combustion index and stable combustion characteristics index were increased, which indicated that effective combustion was achieved through co-combustion.

Kluska *et al.* (2020) studied the co-combustion of pelletized leather tannery waste and hardwood pellets on a grate. It was found that doping wood pellets with tannery waste does not significantly affect the combustion velocity of the fuel mixture and has no significant impact on the temperature front velocity, but an increasing the percentage of leather pellets in the mixture increase the thickness of the ash layer. Ndibe *et al.* (2015) blended biomass with coal and found that the addition of biomass reduced emission of pollutants such as SO_2 and NO_x.

Compared with municipal waste, industrial waste has the characteristics of difficult degradation and pollution, while industrial waste such as leather has a higher heat value than MSW (Li *et al.* 2021). In view of the problem of high moisture content and low calorific value of MSW, the introduction of industrial solid waste into domestic waste incineration can reduce the amount of industrial solid waste and make up for the lack of calorific value of domestic waste. Thus, MSW incineration has great potential for blending industrial solid waste to treat this type of waste (Xu *et al.* 2023).

The current research on the blending of MSW is mostly about the influence of a single factor on the combustion effect, which cannot provide comprehensive guidance for the actual production process. There has been a lack of research on blending leather with MSW. This paper is the first to validate such simulation results using experimental data to ensure the accuracy of the model. A multi-gradient simulation of the MSW leather blending process was simulated to analyze the comprehensive impact factors of the blending process and proposed an optimization plan for MSW blending.

EXPERIMENTAL

The object of this study is a 500t/d capacity Mitsubishi reciprocating mechanical grate furnace. The size is 7.50 m × 9.48 m, with the waste heat boiler of 50 t/h evaporation capacity, and the physical model and grid division is shown in Fig. 1. The wall surface is adiabatic wall, and the wall temperature is set to a gradient distribution according to the change in flue temperature. An unstructured grid is used, and it is encrypted for the area near the secondary air where the flow field changes drastically. The other grids are structured. The total number of grids is about 1.8 million, and the grid irrelevance test has been completed before calculation to ensure that the calculation result is not affected by the number of grids.

The waste materials used in the study came from municipal solid waste in a city in southern China, and the leather was the leftover trimmings from the production of a local shoe factory. The components in the MSW are shown in Table 1. The proximate analysis, elemental analysis, and lower heating value (LHV) of MSW and leather are shown in Table 2. The LHV was determined by experimental methods using the HC-6 heat value analyzer.

Table 1. Components and Proportions in MSW

Components	Soil	Metal	Paper	Plastic	Cloth	Glass	Wood	Food waste
Content (wt%)	6.33	0.52	9.71	31.91	6.38	2.49	4.19	38.47

Table 2. Proximate Analysis and Ultimate Analysis of Sample

Sample	Proximate Analysis (wt%.ar)				Ultimate Analysis (wt%.daf)						LHV (kJ/kg)
	M	V	A	FC	C	H	O*	N	S	Cl	
MSW	48.26	35.01	13.53	3.20	21.14	2.99	13.37	0.55	0.09	0.07	7792
Leather	12.55	69.41	6.03	12.01	42.27	6.09	19.64	12.02	1.09	0.31	22793

Note: M-moisture; V-volatile matter; FC-fixed carbon; A-ash
* By difference

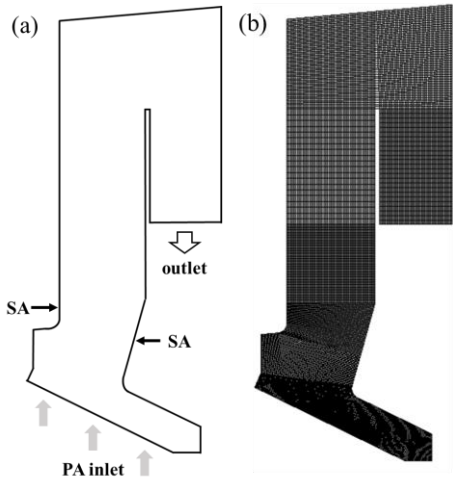

Fig. 1. Schematic diagram of the furnace model. (a) Furnace structure; (b) Mesh division diagram. PA and SA are the primary and secondary air inlets, respectively

Mathematical Model

The combustion of MSW on the grate involves the solid-phase reaction in the grate bed and the gas-phase reaction in the furnace (Gu *et al.* 2022a; Xia *et al.* 2021; Zhou *et al.* 2021). The solid-phase combustion process in the bed is divided into three stages, as shown in Fig. 2: moisture evaporation, volatile matter release, and char combustion (Lee *et al.* 2003).

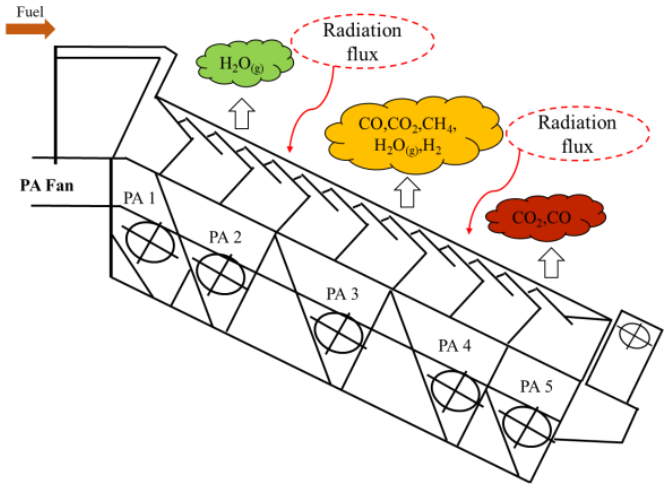

Fig. 2. Diagram of grate furnace operation

Bed Solid Phase Conservation Equation

The bed solid-phase combustion process was simulated by FLIC software. The continuity equation, momentum equation, mass equation, component transport equation, and radiative heat exchange equation of the waste incineration process were referenced from the literature, and the bed solid-phase mass, momentum, energy, and substance concentration conservation equations are shown in Eqs. 1 through 3 (Xu *et al.* 2018),

Continuity equation:

$$\frac{\partial \rho_{sb}}{\partial t} + U_b \frac{\partial \rho_{sb}}{\partial x} + \frac{\partial (\rho_{db} V_s)}{\partial y} = -S_s \quad (1)$$

Energy conservation equation:

$$\frac{\partial \rho_{sb} H_s}{\partial t} + U_b \frac{\partial (\rho_{sb} H_s)}{\partial x} + \frac{\partial (\rho_{sb} V_s H_s)}{\partial x} = \frac{\partial}{\partial_x}\left(\lambda_s \frac{\partial T_s}{\partial x}\right) + \frac{\partial}{\partial_y}\left(\lambda_s \frac{\partial T_s}{\partial y}\right) - S_a h'_s (T_s - T_g) + \sum \Delta h_k \quad (2)$$

Species equation:

$$\frac{\partial (\rho_{sb} Y_{si})}{\partial t} + U_b \frac{\partial (\rho_{sb} Y_{si})}{\partial x} + \frac{\partial (\rho_{sb} V_s Y_{si})}{\partial y} = \frac{\partial}{\partial_x}\left(D_s \frac{\partial (\rho_{sb} Y_{si})}{\partial x}\right) + \frac{\partial}{\partial_y}\left(D_s \frac{\partial (\rho_{sb} Y_{si})}{\partial y}\right) \quad (3)$$

where ρ is density, kg • m^{-3};sb is the bulk density kg • m^{-3}; V is the volatile material in the solid; S_s is the solid mass loss rate; H is the enthalpy, kJ; T is temperature, K; S_a is the particle surface area, m^2; λ is thermal conductivity; Δh_k is the thermal effect of the kth process or reaction, W • m^{-3}; Y is component mass fraction; and D is the mass diffusion coefficient, m^2 • s^{-1}.

For the gas phase of the bed, the conservation equations are referenced in the literature (Pyle and Zaror 1984; Yang *et al.* 2003),

Continuity equation:

$$\frac{\partial (\Phi \rho_g)}{\partial t} + \frac{\partial (\Phi \rho_g U_g)}{\partial x} + \frac{\partial (\Phi \rho_g V_S)}{\partial y} = S_s \quad (4)$$

x-directional momentum:

$$\frac{\partial (\Phi \rho_g U_g)}{\partial t} + \frac{\partial (\Phi \rho_g U_g U_g)}{\partial x} + \frac{\partial (\Phi \rho_g V_g U_g)}{\partial y} = -\frac{\partial P_g}{\partial x} + F(U_g) \quad (5)$$

y-directional momentum:

$$\frac{\partial (\Phi \rho_g V_g)}{\partial t} + \frac{\partial (\Phi \rho_g U_g V_g)}{\partial x} + \frac{\partial (\Phi \rho_g V_g V_g)}{\partial y} = -\frac{\partial P_g}{\partial y} + F(V_g) \quad (6)$$

Energy conservation equation:

$$\frac{\partial (\Phi \rho_g H_g)}{\partial t} + \frac{\partial (\Phi \rho_g U_g H_g)}{\partial x} + \frac{\partial (\Phi \rho_g V_g H_g)}{\partial y} = \frac{\partial}{\partial x}\left(\lambda_g \frac{\lambda T_g}{\partial x}\right) + \frac{\partial}{\partial y}\left(\lambda_g \frac{\lambda T_g}{\partial y}\right) + S_a h'_s (T_s - T_g) + \sum \Delta h_k \quad (7)$$

Species equation:

$$\frac{\partial (\Phi \rho_g Y_{gi})}{\partial t} + \frac{\partial (\Phi \rho_g U_g Y_{gi})}{\partial x} + \frac{\partial (\Phi \rho_g V_g Y_{gi})}{\partial y} = \frac{\partial}{\partial x}\left(D_g \frac{\partial (\Phi \rho_g Y_{gi})}{\partial x}\right) + \frac{\partial}{\partial y}\left(D_g \frac{\partial (\Phi \rho_g Y_{gi})}{\partial y}\right) + S_{sj} + S_{gj} \quad (8)$$

where P is the pressure, Pa; S is the mass source term, kg • m^{-3} • s^{-1}; S_s is the solid mass loss rate, kg • m^{-3} • s^{-1}; Y_{gi}, kg • m^{-3} • s^{-1};S_{gj} is the mass source of gas species; i is solid in species, *i.e.*, moisture, volatile matter, fixed carbon, and ash; j is O_2, CO_2, NH_3, NO, N_2, H_2, C_mH_n, and H_2O in the gas; s is the solid phase.

Radiation Model

Radiation plays a vital role in the fuel combustion process, and the P-1 model was used to solve for the incident radiation of a gas-solid two-phase mixture and then assign the radiation enthalpy source to each phase (El-Sayed and Noseir 2019),

$$\nabla\left(\frac{1}{3a}\nabla G\right) - aG + 4a\sigma T^4 = 0 \quad (9)$$

$$a = \alpha_g a_g + \alpha_s a_s \quad (10)$$

$$S_q = \alpha_q a_q (G - 4\sigma T_q^4) \quad (11)$$

where a is the absorption coefficient; α is the volume fraction; T is the temperature; σ is the Stephan Boltzmann constant. The solid-phase absorption coefficient was calculated from Eq. 12 using the plus GSGGM model (weight-sum-of-gray-gases model) for the gas phase.

$$a_s = -\frac{\ln(1-\varepsilon)}{d_s} \quad (12)$$

Numerical Method

The bed model established by the FLIC program was used for the bed solid-phase combustion, and parameters such as gas temperature, velocity distribution, and component mass fraction were obtained. The parameters were directly interfaced with Fluent software, and the mass and energy data derived from FLIC were imported into Fluent as the boundary conditions for gas-phase combustion. The numerical simulation of bed solid-phase combustion were referenced from Yang *et al.* (2007) and Zhou *et al.* (2005). In this paper, the following assumptions are made: (1) The bed can be regarded as a continuous porous medium; (2) The solid phase consists of moisture, volatile matter, fixed carbon and moisture; (3) The bed moves forward with a constant velocity under the action of a vibrating grid; (4) The parameters are uniformly distributed along the bed width direction; (5) The waste combustion process includes moisture evaporation, volatile analysis and extraction, gas combustion, and char oxidation; (6) The model gases included in the model are CH_4, CO, CO_2, H_2, O_2, H_2O, and N_2. Based on the comprehensive consideration of the applicability of each mechanistic equation, R1-R4 are determined as the gas-phase reaction equations, and the specific parameters are shown in Table 3.

Table 3. Reaction of Finite-Rate/Eddy-Dissipation Concept Model

No.	Reaction	A_r	E_r (J/kmol)	Rate exponent
R_1	$CH_4+0.5O_2\rightarrow CO+2H_2$	5.012×10^{11}	2.000×10^{8}	$[CH_4]$:0.8;$[O_2]$:0.8
R_2	$CH_4+1.5O_2\rightarrow CO+2H_2O$	5.012×10^{11}	2.000×10^{8}	$[CH_4]$:0.8;$[O_2]$:0.8
R_3	$CO+0.5O_2\rightarrow CO_2$	2.239×10^{12}	1.702×10^{8}	[CO]:1;$[O_2]$:0.25
R_4	$H_2+0.5O_2\rightarrow H_2O$	9.870×10^{8}	3.100×10^{7}	$[H_2]$:1;$[O_2]$:0.5

Note: A_r: pre-exponential factor; E_r: activation energy

Numerical simulations of gas-phase combustion in furnace were performed using the double precision solver of the finite element analysis software ANSYS Fluent. The standard k-ε model, the Finite-Rate/Eddy-Dissipation concept of the Species Transport model, and the P-1 radiation model were used, respectively. The equations for density, momentum, turbulence, components, and energy are solved in second order upwind. The grate along-range inlet and SA inlet types are Mass Inlets and the flue outlet is a pressure outlet. The gas temperature, velocity, and component concentration calculated by the FLIC

program are boundary conditions. Then the top radiation temperature distribution from the furnace combustion simulation results is substituted back to FLIC and iterated until the two processes converge.

RESULTS AND DISCUSSION

Experimental Verification

The same parameters were selected for the actual operation as for the simulation. The simulation results were compared with the experimental results to ensure the reliability of the model used. As Table 4 shows, the errors between simulated temperature values and actual measured values at the left side of furnace chamber, the left side of inlet of waste heat boiler, the left side of first radiation channel, and the exit of first radiation channel were 3.81%, 3.98%, 3.68%, and 4.83%, respectively. The error of O_2 content was 12.33%. The location of the measurement points may cause this difference. The measured values are taken from flue gas channel outside the chimney, while the simulated are the furnace chamber outlet. The incinerator was operated under negative pressure conditions, and air leakage led to a high molar fraction of O_2. In summary, the errors between the numerical simulation results and the experimental results were within the permissible range. The model can reflect the actual operation considering the fluctuation of field operating conditions and the idealization of simulated conditions, which establishes the reliability of the mathematical physical model. The model can accurately simulate the processes of flue gas flow, combustion, heat, and mass transfer in the furnace during waste incineration.

Table 4. Comparison of Fuel Parameter Simulation and Experimental Results

Parameters	Experimental Value	Simulation Value	Deviation (%)
Left side of the furnace chamber/(K)	1365	1313	3.81
Left side of waste heat boiler inlet/(K)	1358	1412	3.98
Outlet of the first radiation channel/(K)	1331	1282	3.68
Outlet of the first radiation channel/(K)	1222	1281	4.83
O_2 concentration/(mg/m^3)	6.57	5.76	12.33
CO concentration/(mg/m^3)	10.73	0.3456	—

Effect of Leather Blending Ratio on Co-firing

Compared with municipal waste, leather has a higher volatile content and heat value, as can be seen in Table 2. The LHV of leather is 22793 kJ/kg, and the volatile content is 69.41%, which is much higher than the level in MSW. Moreover, the content of combustible components such as C and H is also higher in the ultimate analysis of leather, so blending leather in MSW can significantly improve the heat value of the mixed fuel. An experimental study of biomass and coal blending in a drop tube furnace was conducted, and it was found that increasing the proportion of biomass improved combustion efficiency (Wang *et al.* 2015). Figure 3(a)(b) shows the temperature distribution in vertical section of furnace center and temperature distribution at different height section of furnace for different ratio of leather blending condition, respectively. It can be seen that with the increase of leather blending ratio, the flame temperature increases gradually, and the area covered with high temperature in furnace increases significantly. However, under the condition of 20% blending ratio, the temperature of the rear wall of the furnace is higher,

which will be a threat to the safe operation of the boiler. Figure 3(c) shows the maximum temperature in the furnace, respectively. When single MSW is burned, the overall temperature in furnace is at a low position, and the maximum temperature in furnace is 1673 K. This is a result of the lower heat value of the mixed fuel. With the increase of the leather blending ratio, the maximum temperature in furnace is 1721K at 10% blending ratio, and the flame height is significantly higher than that of the unblended condition. When continuing to increase the proportion of blending, the flame appears to stick to the rear wall, and the high temperature area to the rear wall will lead a risk of coking. Figure 3(d) shows the average temperature in different heights. It can be seen that changing the leather blending ratio had a great effect on the temperature of the combustion zone, with a maximum temperature change of 200 K, and this effect gradually diminishes in the flue. For leather blending conditions, the proportion control in about 10% had a better combustion effect.

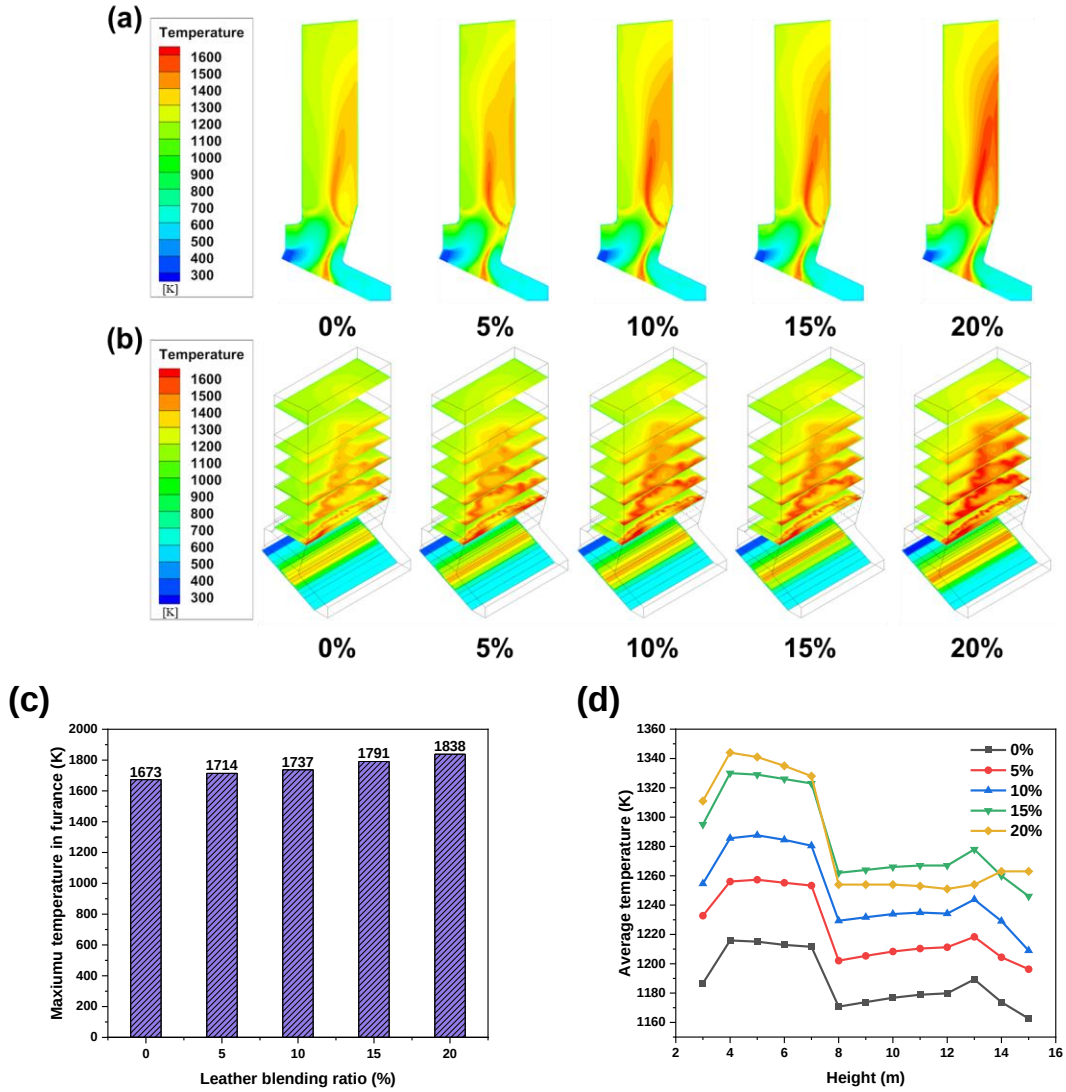

Fig. 3. Furnace chamber temperature simulation results. (a) Temperature distribution in vertical section of furnace center;(b) Temperature distribution at different height section of furnace;(c) Maximum temperature in furnace;(d) Average temperature at different heights

Effect of Ratio of PA and SA on the Co-firing

The ratio of PA and SA affects the effect of solid phase combustion on the bed and gas phase combustion in the furnace. Yang *et al.* (2022) studied the impact of different air supply methods (such as different ratios of PA and SA, ratio of secondary air guns, supply methods of over-fired air), and concluded that the optimal balance of PA and SA is 0.75:0.25. Figure 4(a) shows the gas temperature above the bed.

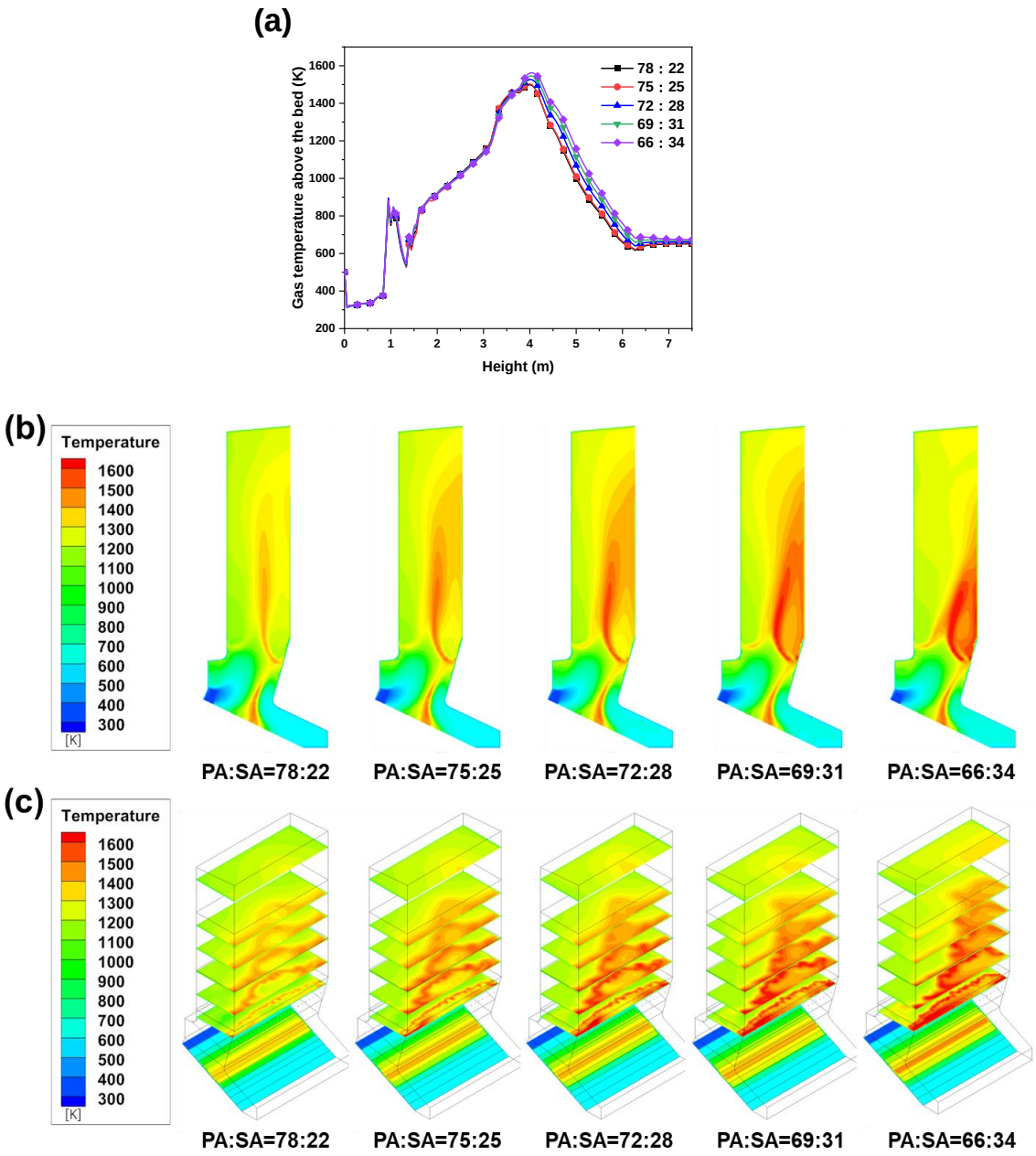

Fig. 4. Furnace chamber temperature simulation results. (a) Temperature distribution in vertical section of furnace center; (b) Temperature distribution at different height section of furnace; (c) Gas temperature above the bed

There was no significant difference in the gas temperature above the bed in the drying stage and volatile fraction release stage under the conditions of leather blending, but in the combustion section, the increase of primary air volume reduced the combustion temperature of coke, leading to a decrease in the temperature of the flue gas produced by on bed.

Figure 4(b)(c) shows the temperature distribution in vertical section of furnace center and temperature distribution at different height section of furnace with 10% leather blending condition, respectively, the SA ratio increases from 0.22 to 0.28, the flame height and the highest temperature in the combustion zone were significantly increased. Because more the SA volume enhanced the turbulence of the combustion zone in furnace, it also extended the flue gas residence time, making the combustion more adequate. By continuing to increase the proportion of secondary air, the extent of the turbulent zone in furnace increased, which led to a less controlled combustion position, and it can be seen in the figure that the high temperature zone starts to shift near the back wall. Therefore, the integrated solid-phase combustion and gas-phase combustion process, the ratio of PA and SA was more appropriate at 72:28.

Effect of Total Air Volume on Leather Blending

The PA mainly provides heat for the evaporation, pyrolysis, and combustion, and it drives the volatile fraction produced into the furnace chamber; the SA is generally of higher velocity, mainly to form turbulent flow in the furnace to make the gas components mix more uniformly and increase the residence time, and the secondary air also provides a large amount of O_2 to promote combustion (Song *et al.* 2020).

Figure 5(a)(b) shows the temperature distribution and temperature contour in the vertical section of furnace center with condition of 10% leather blending respectively. It can be seen that the change in the total air volume did not change the flame position, and it can be seen from the gas produced in the bed that increasing the total air volume caused the gas temperature to go down, which may be a cooling effect from the excess primary air. With the increase of the total air volume, the flame center temperature exhibited a small decrease.

The flame temperature was about 1550 K in condition of 62910 m^3, while with 69900 m^3 working condition the flame was only about 1500 K, about 50 K down. The increase of secondary air made a greater contribution, because the secondary air is room temperature, excessive secondary air and will reduce the furnace chamber temperature, thus reducing the effect of combustion.

Figure 5(c) shows the temperature distribution at different height section of furnace, it can be seen that the furnace chamber temperature decreases with the increase of the total air volume, and when the air volume is higher than 69900 m^3, the decay in temperature in the flue is accelerated, Therefore, the overall temperature of the furnace chamber is the highest when the total air volume of PA and SA is 62910 m^3 when combusting a blend with 10% leather.

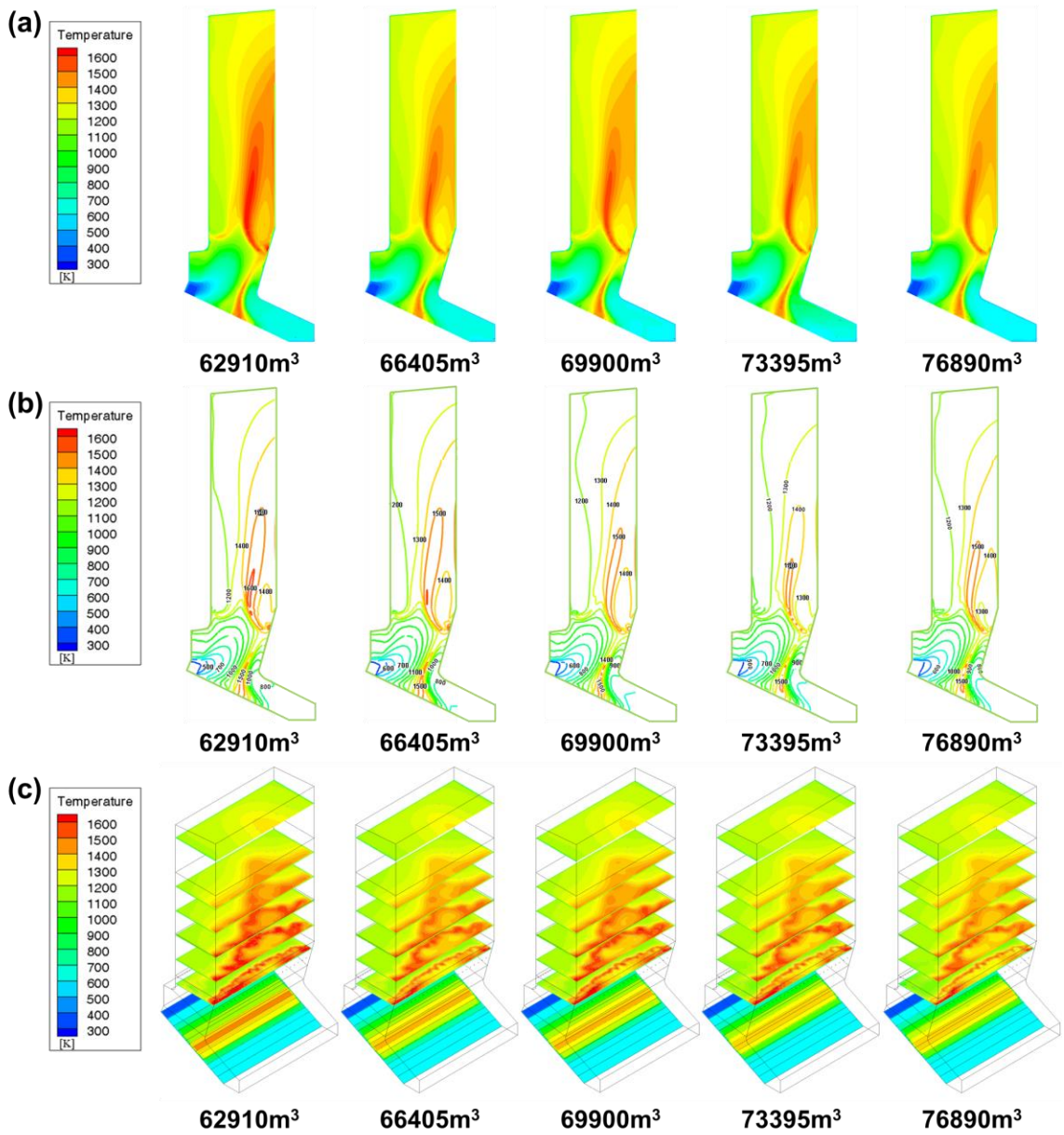

Fig. 5. Furnace chamber temperature simulation results. (a) Temperature distribution in vertical section of furnace center;(b) Temperature contour in vertical section of furnace center;(c) Temperature distribution at different height section of furnace

Effect of Fuel Feed Rate on Leather Blending

The effect of waste combustion on the grate mainly depends on three factors: fuel layer thickness, air supply, and grate movement speed. The feed volume will directly affect the fuel layer thickness (Ke *et al.* 2023; Ma *et al.* 2023). Figure 6(a)(b) shows the temperature distribution of vertical cross-section in the center of the furnace and the temperature distribution at different heights in the vertical direction of the furnace respectively. Under the condition of blending 10% leather, the temperature in the furnace is low when the feed volume is 400 t/d, and the temperature in the main combustion zone is around 1350 K, which is due to the insufficient fuel to maintain the high temperature environment in the furnace.

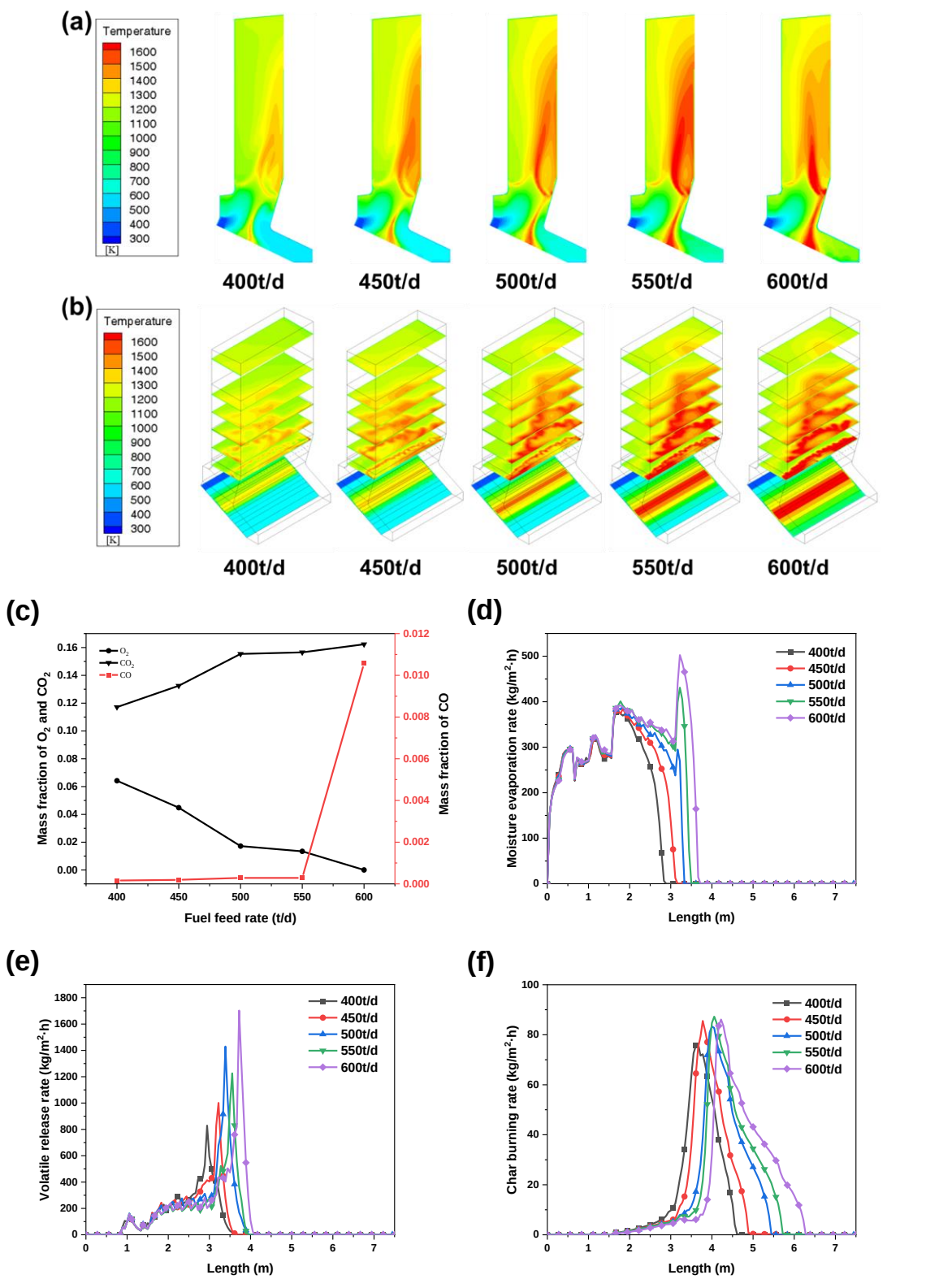

Fig. 6. Simulation results of temperature in furnace and gas mass fraction at the furnace outlet. (a) Temperature distribution of the vertical section in the center of the furnace;(b) Temperature distribution of the horizontal section at different heights in the vertical direction of the furnace;(c) Concentration curve of gas group at the furnace outlet;(d) Moisture evaporation rate;(e) Volatile release rate;(f) Coke burning rate

With the increase of feed quantity to 500 t/d, the flue gas temperature above the bed rises, the temperature of the main combustion zone of the furnace reaches about 1500 K, the combustion range increases, and the flame height is obviously larger than that of the low feed quantity working condition. Increasing the feed amount to 600 t/d, the bed gas temperature continues to rise and the flue gas combustion in the furnace chamber becomes more intense, with the highest temperature rising to 1600 K. However, the flame starts to shift toward the back wall at the feed amounts of 550 t/d and 600t/d, leading to the risk of coking at this location.

Figure 6(c) shows the concentration curve of gas components at the furnace exit. As the feed volume increases from 400 t/d to 500 t/d, the CO_2 mass fraction shows an increasing trend, the O_2 mass fraction decreases from 0.064 to 0.017, and the CO mass fraction also increases gradually with the increase of the feed volume. The CO_2 and O_2 mass fractions are basically stable when the feed volume continues to increase to 550 t/d. However, when the amount of fuel increased to 600 t/d, the CO mass fraction at the furnace outlet increased steeply, this indicates that the conditions of 500 t/d have better combustion, which can ensure a better furnace chamber temperature and also avoid the waste of fuel due to insufficient combustion. As Fig. 6(d)(e)(f) shows, moisture evaporation, volatile release, and coke burning delayed with the fuel feed rate increase, this will compress the reaction time and reduce the response intensity, indicating that the fuel at 600 t/d showed strong under combustion. 10% leather blending should be controlled at about 500 t/d.

CONCLUSIONS

Blending of municipal solid waste (MSW) with leather not only solves the problems of high moisture content and low calorific value of MSW, but also improves the incineration characteristics of MSW. For leather, blending also provides a solution for the harmless treatment of leather and saves the investment of separate treatment of leather. In this paper, the effect of each factor on blending is predicted by numerical simulation methods, and the following conclusions are obtained:

1. Numerical simulations were conducted for the co-firing process of MSW and leather in the grate, and the effects of blending ratio, primary and secondary air ratio, total air volume and fuel feed rate on the combustion of leather blending were investigated.
2. With the increase of blending ratio, the maximum temperature in the furnace increased by 48 K, respectively, and the average temperature in the furnace also increased, but excessive blending ratio caused the flame to be against the wall. The best blending ratio of leather was found to be 10%.
3. The best primary and second air ratio is 72:28 when blending 10% leather. Excessive primary airflow will cause the combustion effect to become worse. The whole temperature in the furnace was also reduced, and excessive secondary airflow led to the highest flame temperature. Average temperature in the furnace increased significantly, but the flame was close to the wall. This presents the risk of coking in this area.
4. In the case of constant ratio of primary and secondary air volume, with the increase of total air volume, the integral temperature of the furnace decreased, and the total inlet air volume of 10% leather blending was selected at 62910 m^3.

5. For the waste incinerator employed in this paper, the fuel feed rate should be maintained in the range of 500-550 t/d. When the fuel feed rate was below 500 t/d, the heat load in the furnace chamber could not maintain high temperatures. However, when the fuel feed rate was higher than 600 t/d, the fuel combustion in the furnace was affected by local lack of oxygen, and the temperature in the furnace decreased. The work explores the key influencing factors of co-firing of MSW and leather and could offer theoretical guidance for the operation in engineering practice.

ACKNOWLEDGMENTS

This work was supported by Support Enterprise Technology Innovation and Development Projects of Hubei Province (2021BAB115), Key Research and Development Program of Hubei Province (2021BBA226).

REFERENCES CITED

Duan, N., Li, D., Wang, P., Ma, W., Wenga, T., Zhong, L., and Chen, G. (2020). "Comparative study of municipal solid waste disposal in three Chinese representative cities," *Journal of Cleaner Production* 254, article 120134. DOI: 10.1016/j.jclepro.2020.120134

El-Sayed, S. A., and Noseir, E. H. (2019). "Simulation of combustion of sesame and broad bean stalks in the freeboard zone inside a pilot-scale bubbling fluidized bed combustor using CFD modeling," *Applied Thermal Engineering* 158, article 113767. DOI: 10.1016/j.applthermaleng.2019.113767

Gu, T., Ma, W., Berning, T., Guo, Z., Andersson, R., and Yin, C. (2022a). "Advanced simulation of a 750 t/d municipal solid waste grate boiler to better accommodate feedstock changes due to waste classification," *Energy* 254, article 124338. DOI: 10.1016/j.energy.2022.124338

Gu, T., Ma, W., Guo, Z., Berning, T., and Yin, C. (2022b). "Stable and clean co-combustion of municipal sewage sludge with solid wastes in a grate boiler: A modeling-based feasibility study," *Fuel* 328, article 125237. DOI: 10.1016/j.fuel.2022.125237

Ke, X., Zhu, S., Huang, Z., Zhang, M., Lyu, J., Yang, H., and Zhou, T. (2023). "Issues in deep peak regulation for circulating fluidized bed combustion: Variation of NOx emissions with boiler load," *Environmental Pollution* 318, article 120912. DOI: 10.1016/j.envpol.2022.120912

Kluska, J., Turzyński, T., Ochnio, M., and Kardaś, D. (2020). "Characteristics of ash formation in the process of combustion of pelletised leather tannery waste and hardwood pellets," *Renewable Energy* 149, 1246-1253. DOI: 10.1016/j.renene.2019.10.122

Lee, G. W., Lee, S. J., Jurng, J., and Hwang, J. (2003). "Co-firing of paper sludge with high-calorific industrial wastes in a pilot-scale nozzle-grate incinerator," *Journal of Hazardous Materials* 101, 273-283. DOI: 10.1016/S0304-3894(03)00144-4

Li, Z. S., Zhang, Y. R., Xiong, T., Li, B. L., Xiao, M. H., Xu, X. Z., Hu, R., Zhu, Y., and Li, J. F. (2021). "Preparation of hydrogen-rich gas by catalytic pyrolysis of straw-plastic mixture with nickel-based honeycomb cinder," *BioResources* 16, 223-235.

DOI: 10.15376/biores.16.1.223-235
Lopes, E. J., Queiroz, N., Yamamoto, C. I., and da Costa Neto, P. R. (2018). "Evaluating the emissions from the gasification processing of municipal solid waste followed by combustion," *Waste Management* 73, 504-510. DOI: 10.1016/j.wasman.2017.12.019
Ma, D., Zhang, S., He, X., Zhang, J., and Ding, X. (2023). "Combustion stability and NOX emission characteristics of a 300 MWe tangentially fired boiler under ultra-low loads with deep-air staging," *Energy* 269, article 126795. DOI: 10.1016/j.energy.2023.126795.
Martin, J. J .E., Koralewska, R., and Wohlleben, A. (2015). "Advanced solutions in combustion-based WtE technologies," *Waste Management* 37, 147-156. DOI: 10.1016/j.wasman.2014.08.026
Muralidharan, V., Palanivel, S., and Balaraman, M. (2022). "Turning problem into possibility: A comprehensive review on leather solid waste intra-valorization attempts for leather processing," *Journal of Cleaner Production* 367, article 133021. DOI: 10.1016/j.jclepro.2022.133021
Ndibe, C., Grathwohl, S., Paneru, M., Maier, J., and Scheffknecht, G. (2015). "Emissions reduction and deposits characteristics during cofiring of high shares of torrefied biomass in a 500kW pulverized coal furnace," *Fuel* 156, 177-189. DOI: 10.1016/j.fuel.2015.04.017
Pyle, D. L., and Zaror, C. A. (1984). "Heat transfer and kinetics in the low temperature pyrolysis of solids," *Chemical Engineering Science* 39, 147-158. DOI: 10.1016/0009-2509(84)80140-2
Song, M., Zeng, L., Zhao, Y., Pei, J., and Li, Z. (2020). "Secondary air distribution in a 600 MWe multi-injection multi-staging down-fired boiler: A comprehensive study," *Journal of the Energy Institute* 93, 1250-1260. DOI: 10.1016/j.joei.2019.11.008
Wang, Y. F., Wang, X. B., Hu, Z. F., Li, Y., Deng, S. H., Niu, B., and Tan, H. Z. (2015). "NO emissions and combustion efficiency during biomass co-firing and air-staging," *BioResources* 10, 3987-3998. DOI: 10.15376/biores.10.3.3987-3998
Xia, Z., Long, J., Yan, S., Bai, L., Du, H., and Chen, C. (2021). "Two-fluid simulation of moving grate waste incinerator: Comparison of 2D and 3D bed models," *Energy* 216, article 119257. DOI: 10.1016/j.energy.2020.119257
Xu, H., Li, L., Tang, W., Sun, Z., Chen, Y., Sun, G., Gu, Q., and Duan, L. (2023). "Experimental study on the combustion behavior and NOx emission during the co-combustion of combustible industrial solid wastes," *Journal of the Energy Institute* 106, article 101150. DOI: 10.1016/j.joei.2022.11.010
Xu, J., Liao, Y., Yu, Z., Cai, Z., Ma, X., Dai, M., and Fang, S. (2018). "Co-combustion of paper sludge in a 750 t/d waste incinerator and effect of sludge moisture content: A simulation study," *Fuel* 217, 617-625. DOI: 10.1016/j.fuel.2017.12.118
Yan, M., Tian, X., Antoni, Yu, C., Zhou, Z., Hantoko, D., Kanchanatip, E., and Khan, M. S. (2021). "Influence of multi-temperature primary air on the characteristics of MSW combustion in a moving grate incinerator," *Journal of Environmental Chemical Engineering* 9, article 106690. DOI: 10.1016/j.jece.2021.106690
Yang, X., Liao, Y., Ma, X., and Zhou, J. (2022). "Effects of air supply optimization on NOx reduction in a structurally modified municipal solid waste incinerator," *Applied Thermal Engineering* 201, article 117706. DOI: 10.1016/j.applthermaleng.2021.117706

Yang, Y. B., Newman, R., Sharifi, V., Swithenbank, J., and Ariss, J. (2007). "Mathematical modelling of straw combustion in a 38MWe power plant furnace and effect of operating conditions," *Fuel* 86, 129-142. DOI: 10.1016/j.fuel.2006.06.023

Yang, Y. B., Yamauchi, H., Nasserzadeh, V., and Swithenbank, J. (2003). "Effects of fuel devolatilisation on the combustion of wood chips and incineration of simulated municipal solid wastes in a packed bed," *Fuel* 82, 2205-2221. DOI: 10.1016/S0016-2361(03)00145-5

Zhang, J. H., Yang, H., Zhang, G. Y., Kang, G. J., Liu, Z. E., Yu, J., and Gao, S. Q. (2022). "Research on the influence of combustion methods on NOx emissions from co-combustion of various tannery wastes," *ACS Omega* 7, 4110-4120. DOI: 10.1021/acsomega.1c05640

Zhou, A., Xu, H., Meng, X., Yang, W., and Sun, R. (2021). "Development of a numerical model for co-combustion of the blended solid waste fuel in the grate boiler," *Chemical Engineering Journal* 405, article 126604. DOI: 10.1016/j.cej.2020.126604

Zhou, H., Jensen, A. D., Glarborg, P., Jensen, P. A., and Kavaliauskas, A. (2005). "Numerical modeling of straw combustion in a fixed bed," *Fuel* 84, 389-403. DOI: 10.1016/j.fuel.2004.09.020.

Article submitted: March 5, 2023; Peer review completed: March 25, 2023; Revised version received and accepted: April 2, 2023; Published: April 7, 2023.
DOI: 10.15376/biores.18.2.3666-3680